

BRIEF COMMUNICATION

Using automated electrode localization to guide stimulation management in DBS

Mikkel V. Petersen¹ , Andreas Husch² , Christine E. Parsons³ , Torben E. Lund¹ , Niels Sunde⁴ & Karen Østergaard⁵ 

¹Center of Functionally Integrative Neuroscience (CFIN), Department of Clinical Medicine, Aarhus University, Nørrebrogade 44, 8000 Aarhus C, Denmark

²National Department of Neurosurgery, Centre Hospitalier de Luxembourg, 4 Rue Ernest Barble, Luxembourg (City), Luxembourg

³Interacting Minds Centre, Department of Clinical Medicine, Aarhus University, Jens Chr. Skous Vej 7, Aarhus C 8000, Denmark

⁴Department of Neurosurgery, Aarhus University Hospital, Nørrebrogade 44, Aarhus C 8000, Denmark

⁵Department of Neurology, Aarhus University Hospital, Nørrebrogade 44, Aarhus C 8000, Denmark

Correspondence

Mikkel V. Petersen, CFIN, Aarhus University Hospital, Building 10G, 4th floor, Nørrebrogade 44, 8000 Aarhus C, Denmark. Tel: +45 21 84 87 97; Fax: +45 78 46 44 00; E-mail: mikkel.petersen@cfin.au.dk

Funding Information

This work was funded by the 'Danish Parkinsons Association' (Parkinsonforeningen), 'Jascha Fond' and by the Fonds National de la Recherché, Luxembourg, Grant AFR 5748689.

Received: 2 February 2018; Revised: 20 April 2018; Accepted: 1 May 2018

Abstract

Deep Brain Stimulation requires extensive postoperative testing of stimulation parameters to achieve optimal outcomes. Testing is typically not guided by neuroanatomical information on electrode contact locations. To address this, we present an automated reconstruction of electrode locations relative to the treatment target, the subthalamic nucleus, comparing different targeting methods: atlas-, manual-, or tractography-based subthalamic nucleus segmentation. We found that most electrode contacts chosen to deliver stimulation were closest or second closest to the atlas-based subthalamic nucleus target. We suggest that information on each electrode contact's location, which can be obtained using atlas-based methods, might guide clinicians during postoperative stimulation testing.

doi: 10.1002/acn3.589

Introduction

A crucial stage of Deep Brain Stimulation (DBS) treatment is postoperative selection of stimulation settings. The overall aim of DBS is to achieve a balance between stimulating structures mediating desired effects, while avoiding structures mediating unwanted side effects.^{1–3} Once the electrode location is fixed, altering stimulation parameters, and consequently the stimulation field, is the only means of fine-tuning treatment outcome. Selecting active electrode contacts and stimulation parameters requires extensive testing of different settings with a trial and error approach.^{3–5}

Postoperative stimulation selection is time-consuming for the clinician and demanding on the patient. It is traditionally performed using mono-polar review, systematically testing all available electrode contacts. This process is currently not informed by neuroanatomical information about the electrode contact locations. There is a clear

question as to whether this could helpfully inform stimulation settings. As segmented electrodes with more contact options, and therefore even greater numbers of parameter configurations emerge, this may become a critical issue.^{6–8} Furthermore, in a subset of patients, poststimulation management is problematic, and may benefit from insights about the patient's-specific neuroanatomical patterns.

There are at least two levels of neuroanatomical information that could be informative in postoperative stimulation planning. The first is a basic mapping of the target and surrounding structures, relative to the final implanted electrode position. The second involves adding connectivity-based mapping of pathways implicated in treatment effects to a basic mapping of structures. Connectivity-based mapping in patients can be done using diffusion weighted imaging (DWI)-based tractography. This *in vivo* technique is increasingly explored in DBS preoperative

planning,^{9–11} and has been highlighted as informative in targeting the STN for Parkinson's disorder.¹² Specifically, these recent studies have argued that targeting of motor cortex to STN pathways, delineated using tractography, is important in achieving optimal treatment outcomes.^{13–16}

To date, the use of neuroanatomical information in postoperative stimulation management has been difficult to achieve because of a lack of automated software tools for clinicians (several manual tools exist, DBSproc, PyDBS, Stimvision, LeadDBS). One toolbox, PaCER (Precise and Convenient Electrode Reconstruction) has been developed to address this.¹⁷ This tool can automatically locate and reconstruct the implanted electrodes accurately. It then generates interactive 3D (PDF) reports, including measurements of Euclidean distances between electrode contacts and structures of interest.¹⁸

Here, we perform a retrospective analysis of DBS electrode locations and stimulation amplitudes relative to the STN, with the STN defined using four methods: (1) an atlas-based (fully automated) segmentation of the STN and (2) an atlas-based motor-STN, (3) a manual segmentation of the STN, and (4) a motor-STN defined for each patient using tractography. We examine the correspondence between the contacts ultimately chosen by clinicians after extensive testing and those suggested by neuroanatomical information. The overarching aim is to explore whether neuroanatomical information can be used to guide contact testing in postoperative stimulation management.

Patients and Methods

Patients

Twelve PD patients (seven male, five female; Mean age = 58 years (STD = 6), UPDRS-III Medication on: M = 11 (STD = 3.6); UPDRS-III Medication off, M = 36.5 (STD = 9.5); UPDRS-III Medication off, Stim on M = 11.7 (STD = 6.3)) undergoing bilateral STN-DBS at Aarhus University Hospital were included. All patients were evaluated by an experienced multidisciplinary team to ensure DBS candidacy and all gave written informed consent. The study was approved by the local ethics committee. All patients were implanted with the Medtronic 3389 lead and treated using mono-polar stimulation (6-month follow-up for 9 patients, 3-month for 2). The frame-based (Leksell) implantation procedure used includes microelectrode recording (five simultaneous tracks) and stimulation testing to finalize the implantation site.

Image acquisition

Two weeks prior to surgery, each patient underwent an extended preoperative MRI session under full anesthesia.

This MRI protocol included conventional T1- and T2-weighted MRI for surgical planning, along with a diffusion-weighted imaging (DWI) acquisition. The DWI data were acquired using a readout-segmented echo-planar imaging sequence allowing high angular (62 directions, $B = 1000 \text{ s/mm}^2$) and spatial resolution (1.4 mm isotropic) with substantially reduced EPI distortions. Detailed acquisition parameters are described in Petersen et al.¹⁹ A CT scan was obtained the day after surgery.

Image processing

The image processing workflow is illustrated in detail in Figure 1. Briefly, the PaCER toolbox (<https://ad-huschi.github.io/PaCER>)^{17,18} was first used to automatically locate individual electrode contacts. Next, the preoperative MRI data were used to (1) automatically warp basal ganglia structures from two high-resolution atlases,^{20,21} (2) manually segment the STN, and (3) delineate the STN-subregion directly connected with motor cortex using probabilistic tractography. Finally, using PaCER we calculated the distances between active contacts chosen and the center-of-gravity of the three defined STN targets (see Figure 2).

First, we correlated these distances with (1) the stimulation voltage applied and (2) the improvement in unilateral UPDRS-III subscores. Second, we ranked the contacts on each lead from 1 to 4, starting with the contact closest to the target structure (Figure 3). We then compared the contacts closest to the target center, as calculated by each of the four methods (atlas-STN, atlas-motor-STN, manual-STN, and tractography-motor-STN) against the actual chosen contacts.

Results

The variability of active contact coordinates was calculated along the lateral-medial (x-) (M = -0.77 mm, SD = 1.67), anterior-posterior (y-) (M = 0.67 mm, SD = 1.45), and inferior-superior (z-) axis (M = 0.02 mm, SD = 1.48) relative to the manual-STN center-of-gravity in a coordinate-system realigned to atlas-space. There was a significant positive correlation between the stimulation amplitude (M = 2.98V, SD = 0.54) at an active contact and the target center-of-gravity, as calculated using the atlas-STN (M = 2.29 mm, SD = 1.17; Pearson's $r = 0.43$, $P = 0.04$) and the manual-STN methods (M = 2.44 mm, SD = 1.22; Pearson's $r = 0.52$, $P = 0.01$), but not for the atlas-motor (M = 2.30 mm, SD = 1.04; Pearson's $r = 0.20$, $P = 0.36$) or the tractography-motor-STN (M = 2.37 mm, SD = 1.25; Pearson's $r = 0.40$, $P = 0.06$, see Supporting Information for a discussion on lead placement distances). In our sample ($N = 12$), we therefore

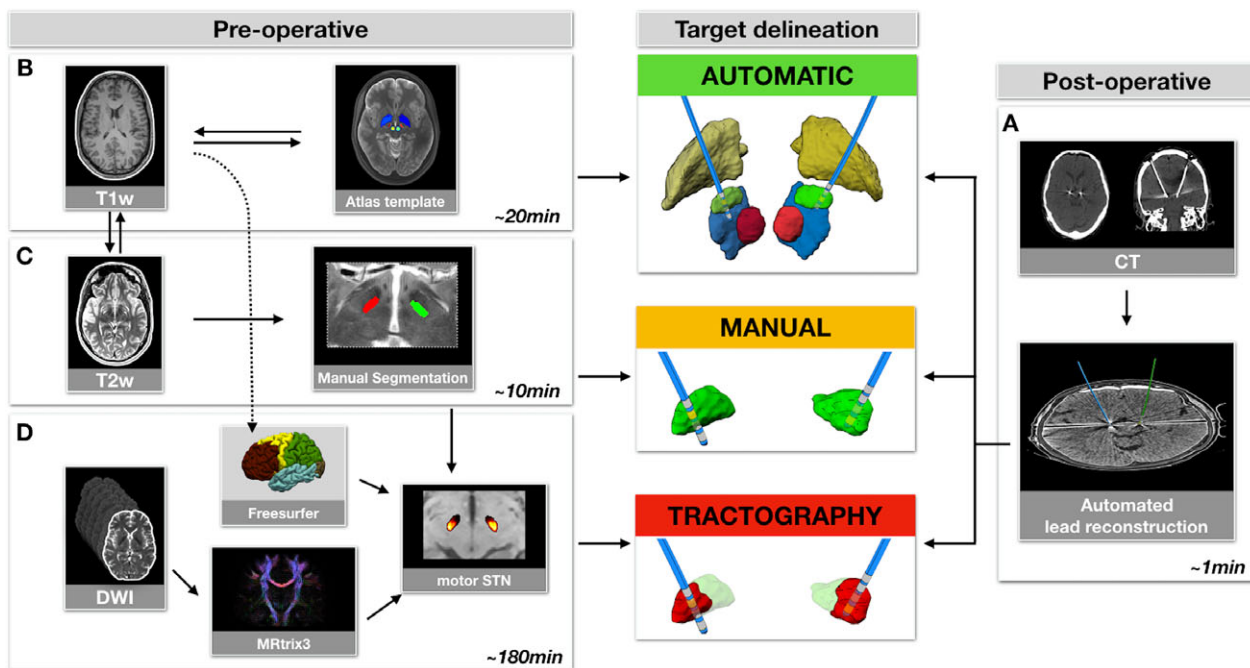


Figure 1. Flowchart illustrating the processing workflow. (A) The PaCER toolbox (in revision) was used to accurately reconstruct DBS electrodes using postoperative CT data. (B) An automated pipeline within PaCER (in review) was used to rigidly coregister intrasubject scans (FSL-Flirt) and nonlinearly transform basal ganglia structures from atlas- to patient-space (ANTs). (C) The T2w scan was upsampled to a 0.5 mm isotropic resolution and used to manually segment the STN (ITKsnap). (D) First, the T1w scans were used to parcellate the frontal lobe into one motor cortex (MC; supplementary, pre- and primary motor cortex) and one prefrontal (PF) region (Freesurfer). Next, the DWI data were preprocessed (de-noising, gibbs-correction, combined motion- and eddy-current correction and intensity inhomogeneity correction) and a higher order diffusion model was fitted using constrained spherical deconvolution (MRtrix3). Finally, tractography was performed using a probabilistic algorithm (iFOD2); streamlines were seeded from the STN segmentation (500 seeds/voxel), those connecting directly with the ipsilateral MC and PF were extracted and resampled to track density maps allowing calculation of the ratio between MC and PF connections across STN voxels. The maps were thresholded in a winner-takes-all approach to define a STN-subregion consisting of voxels dominated by MC connectivity (50% streamlines connecting with MC).

find evidence to suggest that the closer the active contact is to the center of the (atlas or manual) STN, the less voltage is applied to achieve therapeutic benefit.

To examine effects on clinical improvement, we correlated unilateral UPDRS-III change subscores and distance from the (contralateral) STN center for both the left and right hemisphere electrode contacts. We found no correlation between clinical improvement and any of the calculated STN target centers (all r 's < 0.19 , P 's > 0.40).

Next, we ranked the electrode contacts based on their proximity to the STN target structures. For the atlas-STN and atlas-motor-STN, we found that 58% and 50% of the active contacts were closest to the target center-of-gravity, respectively. For the manual and tractography-motor STN, 38% and 36% of the active contacts were closest. The most distant contact from the calculated center-of-gravities was never chosen to deliver stimulation (see Table S2).

Discussion

We present a retrospective analysis of the location of active electrodes relative to the DBS target, the STN, delineated using four different methods (atlas-based STN, atlas-based motor-STN, manual-STN, tractography-motor STN). First, we found a significant positive correlation between the stimulation amplitude applied and the electrode contact's proximity to the center of the STN, as defined using the automatic and manual-segmentation methods. Second, we found that the majority of electrode contacts chosen to deliver stimulation were closest or second closest to the target center-of-gravities, defined using any of the four methods. We suggest that information on each electrode contact's location might be useful in guiding clinicians during postoperative stimulation testing.

We used four methods to define the STN target, each with advantages and disadvantages. An automatically estimated STN does not require manual input, but may not

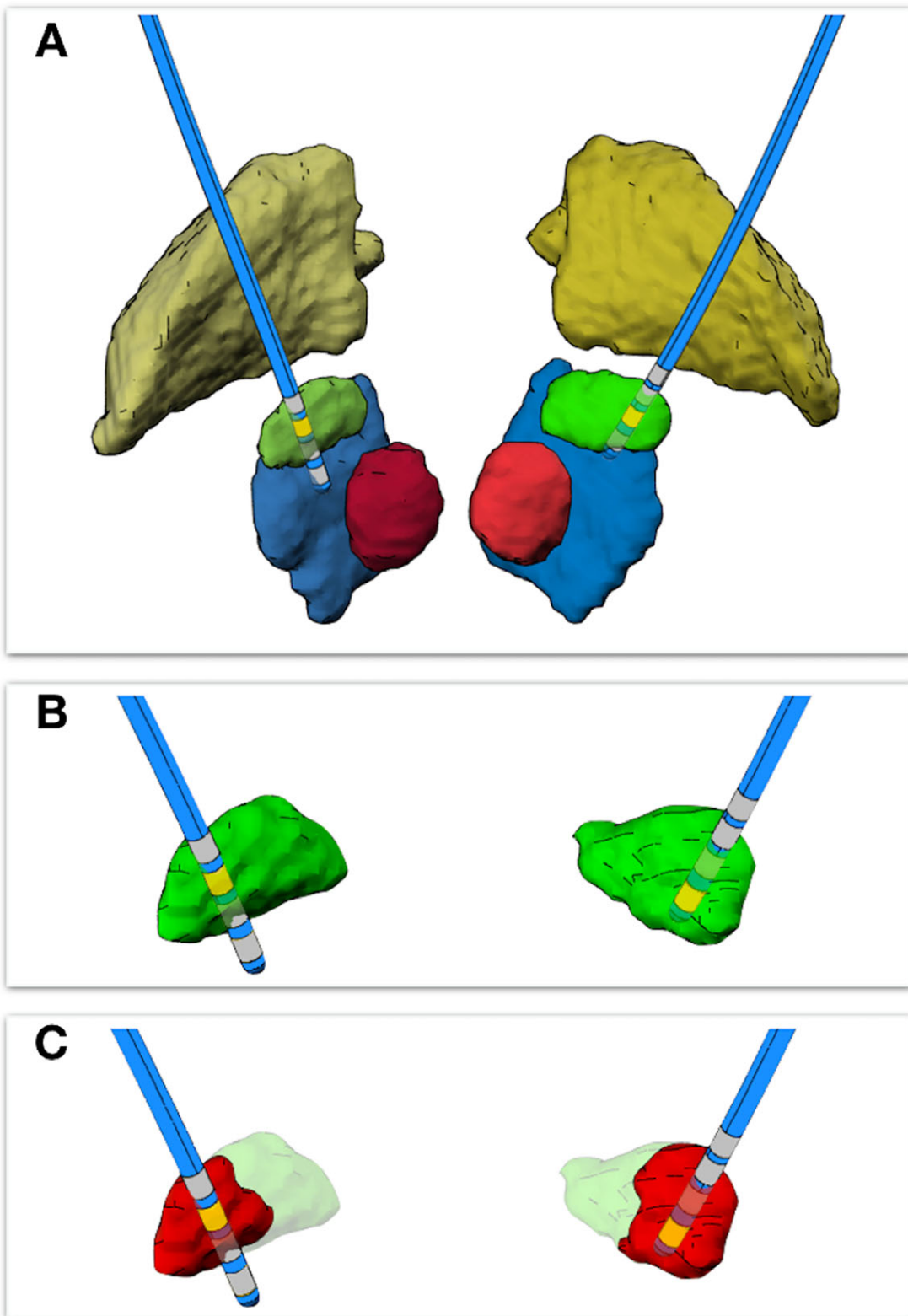


Figure 2. DBS electrodes plotted with (A) automatically estimated basal ganglia structures (based on high-resolution atlas data), (B) manual-STN segmentation (green), and (C) tractography-derived motor segment (red). Yellow contact highlights the one located closest to the target center-of-gravity. Depicted basal ganglia structures: Yellow = Globus Pallidus. Blue = Substantia Nigra. Red = Red Nucleus.

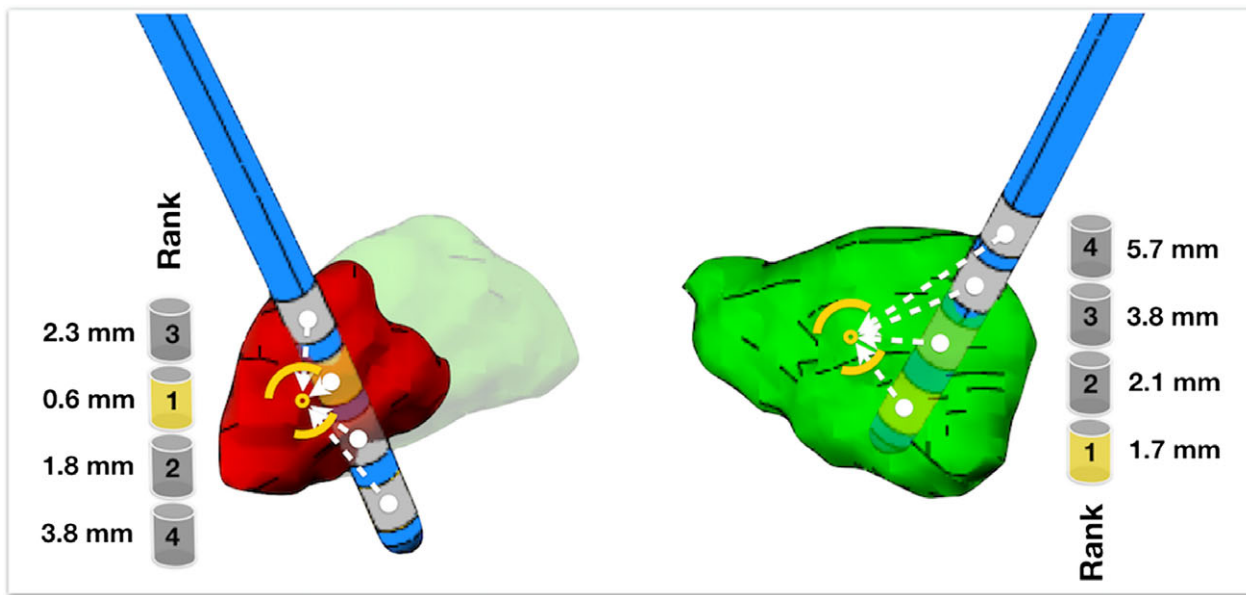


Figure 3. Illustration of distances calculated between each contact and the center-of-gravity of the target structures. Cylinders illustrate the ranking of contacts based on contact-target distances. Left = motor segment, Right = Manual-STN.

be as accurate as the manually segmented STN (however, see 22). The motor segment of the STN has been strongly implicated in treatment benefit, but the tractography analysis required to delineate it depends on technical expertise, and is not without limitation (see 19,23). Using both the automatic and manually segmented methods, we found an association between the stimulation voltage applied and proximity of the active contact to the entire STN. We suggest that an automatic method may be adequate for delineating the STN, at least in this context. We did not find an association between the stimulation applied and contact proximity to the tractography- or to the atlas-based motor-STN. While there is a general consensus that a region of the STN directly connected with cortical motor regions is a 'hot spot' for treatment effects,^{14–16,24,25} we argue that there may be challenges in using tractography to accurately delineate this small sub-region.^{19,26} Indeed, another recent study has noted unacceptable error margins using template-derived (group atlas) tractography for DBS tremor targeting, compared with patient-specific probabilistic tractography.²⁷

Our findings on the importance of electrode contact locations will be of no surprise to clinicians. However, our novel contribution is in demonstrating that new, open-source tools can be used to easily integrate detailed multimodal neuroimaging data into clinical practice, thereby opening avenues for future research. We suggest that our findings on the importance of electrode contact locations open an important avenue for further research. We found that most of the electrode contacts chosen after

extensive, systematic testing were either closest or second closest to the STN center-of-gravity. If our results are replicated in a prospective study, we believe that clinicians can use this information to guide postoperative stimulation testing. For instance, knowing that an electrode contact is furthest from the theoretical 'optimal' target, clinicians may choose to focus testing efforts on the remaining contacts. Using neuroanatomical information to guide or constrain testing may become even more critical when innovations, such as segmented electrodes, become more commonplace.^{6–8}

There were several limitations to our current study. First, our sample size was small ($N = 12$) which may explain in part our null findings for the motor-STN/contact distance and for the UPDRS-III subscores/electrode contact locations. Second, we used a CT scan taken 1 day postoperatively, and this may be impacted by unresolved brain shift. Third, we did not correct for susceptibility-induced distortions, but we did use the time-consuming RESOLVE sequence, designed to address this. Finally, our analyses concerning stimulation amplitude (voltage) are simplified, and do not take into account factors such as impedance, tissue anisotropy, or axon diameter.²⁶ We also use the outcomes from clinical programming (electrode contact chosen or not); it is possible that clinicians did not chose the optimal contact for stimulation. Notwithstanding these limitations, we present a novel analysis combining pre- and postoperative patient data, using the most current toolboxes available (PaCER^{17,18}) and multiple methods for defining our DBS target structure.

Much of the recent DBS research has focused on improving preoperative targeting. However, postoperative stimulation management is also fundamental to achieving good treatment outcome and may be guided by neuroanatomical information. As automated tools such as PaCER emerge, this becomes increasingly feasible to use systematically in the clinic. We suggest a need for prospective studies, with larger samples, comparing neuroanatomically informed stimulation with traditional, monopolar review procedures.

Acknowledgments

Mikkel V. Petersen was supported by the Danish Parkinson Association and Jascha Fonden. Andreas Husch was supported by the Fonds National de la Recherché, Luxembourg, Grant AFR 5748689. Christine E. Parsons was supported by TrygFonden. Torben E. Lund was supported by the Danish Ministry of Science, Technology and Innovation's UNIK program (MINDLab). Karen Østergaard was supported by the Lundbeck Foundation, the Danish Research council for Independent Research, the Danish Parkinson Association, the Central Denmark Research Foundation, Aarhus University and Aarhus University Hospital. The 3T Magnetom Tim Trio was funded by a grant from the Danish Agency for Science, Technology and Innovation.

Author Contributions

MVP was involved in all stages of this article. AH was involved in data processing, statistical analysis, review and critique of manuscript. CEP was involved in concept and design of study, statistical analysis and writing of manuscript. TEL was involved in data acquisition, data processing, review and critique of manuscript. NS was involved in data acquisition, data processing, review and critique of manuscript. KO was involved in concept and design of study, review and critique of manuscript.

Conflict of Interests

Outside of the submitted work, Dr. Østergaard has received personal fees from Medtronic Inc. who manufactures the DBS hardware used at Aarhus University Hospital.

References

1. Benabid AL, Chabardes S, Mitrofanis J, Pollak P. Deep brain stimulation of the subthalamic nucleus for the treatment of Parkinson's disease. *Lancet Neurol*. 2009;8:67–81.
2. Johnson MD, Miocinovic S, McIntyre CC, Vitek JL. Mechanisms and targets of deep brain stimulation in movement disorders. *Neurotherapeutics* 2008;5:294–308.
3. Krack P, Fraix V, Mendes A, et al. Postoperative management of subthalamic nucleus stimulation for Parkinson's disease. *Mov Disord* 2002;17(Suppl 3): S188–S197.
4. Volkmann J, Moro E, Pahwa R. Basic algorithms for the programming of deep brain stimulation in Parkinson's disease. *Movement Disord*. 2006;21:S284–S289.
5. Volkmann J, Herzog J, Kopper F, Deuschl G. Introduction to the programming of deep brain stimulators. *Mov Disord* 2002;17(Suppl 3):S181–S187.
6. Pollo C, Kaelin-Lang A, Oertel MF, et al. Directional deep brain stimulation: an intraoperative double-blind pilot study. *Brain* 2014;137:2015–2026.
7. Kuhn AA, Volkmann J. Innovations in deep brain stimulation methodology. *Movement Disord*. 2017;32: 11–19.
8. embek TA, Reker P, Visser-Vandewalle V, et al. Directional DBS increases side-effect thresholds-A prospective, double-blind trial. *Mov Disord* 2017;32:1380–1388.
9. Schlaepfer TE, Bewernick BH, Kayser S, et al. Rapid effects of deep brain stimulation for treatment-resistant major depression. *Biol Psychiat* 2013 Jun 15;73:1204–1212.
10. Riva-Posse P, Choi KS, Holtzheimer PE, et al. Defining critical white matter pathways mediating successful subcallosal cingulate deep brain stimulation for treatment-resistant depression. *Biol Psychiat* 2014;76:963–969.
11. Coenen VA, Allert N, Paus S, et al. Modulation of the cerebello-thalamo-cortical network in thalamic deep brain stimulation for tremor: a diffusion tensor imaging study. *Neurosurgery* 2014;75:657–669.
12. Avecillas-Chasin JM, Alonso-Frech F, Parras O, et al. Assessment of a method to determine deep brain stimulation targets using deterministic tractography in a navigation system. *Neurosurg Rev* 2015;38:739–751.
13. Accolla EA, Herrojo Ruiz M, Horn A, et al. Brain networks modulated by subthalamic nucleus deep brain stimulation. *Brain* 2016;139(Pt 9):2503–2515.
14. Akram H, Sotiroopoulos SN, Jbabdi S, et al. Subthalamic deep brain stimulation sweet spots and hyperdirect cortical connectivity in Parkinson's disease. *NeuroImage* 2017;158:332–345.
15. Horn A, Reich M, Vorwerk J, et al. Connectivity predicts deep brain stimulation outcome in Parkinson disease. *Ann Neurol* 2017;82:67–78.
16. Vanegas-Arroyave N, Lauro PM, Huang L, et al. Tractography patterns of subthalamic nucleus deep brain stimulation. *Brain* 2016;139(Pt 4):1200–1210.
17. Husch A, Petersen MV, Gemmar P, et al. PaCER - A fully automated method for electrode trajectory and contact reconstruction in deep brain stimulation. *NeuroImage: Clinical*. 2018;17:80–89.

18. Husch A, Petersen MV, Gemmar P, et al. Post-operative deep brain stimulation assessment: automatic data integration and report generation. *Brain Stimulation*. 2018; <https://doi.org/10.1016/j.brs.2018.01.031>.
19. Petersen MV, Lund TE, Sunde N, et al. Probabilistic versus deterministic tractography for delineation of the cortico-subthalamic hyperdirect pathway in patients with Parkinson disease selected for deep brain stimulation. *J Neurosurg* 2017;126: 1657–1668.
20. Wang BT, Poirier S, Guo T, et al. Generation and evaluation of an ultra-high-field atlas with applications in DBS planning. *Proc Spie*. 2016;9784.
21. Ewert S, Plettig P, Li N, et al. Toward defining deep brain stimulation targets in MNI space: a subcortical atlas based on multimodal MRI, histology and structural connectivity. *NeuroImage* 2017;170:271–282.
22. Haegelen C, Coupe P, Fonov V, et al. Automated segmentation of basal ganglia and deep brain structures in MRI of Parkinson's disease. *Int J Comput Ass Rad*. 2013;8:99–110.
23. Maier-Hein KH, Neher PF, Houde JC, et al. The challenge of mapping the human connectome based on diffusion tractography. *Nat Commun* 2017;8:1349.
24. Bot M, Schuurman PR, Odekerken VJJ, et al. Deep brain stimulation for Parkinson's disease: defining the optimal location within the subthalamic nucleus. *J Neurol Neurosurg Psychiatry* 2018;89:493–498.
25. Horn A, Neumann WJ, Degen K, et al. Toward an electrophysiological "sweet spot" for deep brain stimulation in the subthalamic nucleus. *Hum Brain Mapp* 2017; <https://doi.org/10.1002/hbm.23594>.
26. Gunalan K, Chaturvedi A, Howell B, et al. Creating and parameterizing patient-specific deep brain stimulation pathway-activation models using the hyperdirect pathway as an example. *PLoS ONE* 2017;12:e0176132.
27. Akram H, Dayal V, Mahlknecht P, et al. Connectivity derived thalamic segmentation in deep brain stimulation for tremor. *Neuroimage Clin* 2018;18:130–142.

Supporting Information

Additional supporting information may be found online in the Supporting Information section at the end of the article:

Table S1. Raw data on stimulation settings, contact-to-target distances, pre- and postoperative UPDRS improvement (global and unilateral scores).

Table S2. Distribution of active contacts ranked by their proximity to the specified targets (center-of-gravity).

Table S3. Descriptive statistics and correlations.

Table S4. Descriptive statistics and correlations with stimulation Voltage as covariate.

Figure S1. Reconstructed electrodes plotted together with atlas structures in all 12 patients.

Figure S2. Scatter plot illustrating the spread of the active contact relative to the STN (manual) center-of-gravity.

Figure S3. Interactive 3D model of reconstructed electrodes and atlas-based basal ganglia structures.